

Numerical Evaluation of Lateral Diffusion Inside Diffusive Gradients in Thin Films Samplers

Jakob Santner,^{*,†} Andreas Kreuzeder,^{†,‡} Andrea Schnepf,[§] and Walter W. Wenzel[†]

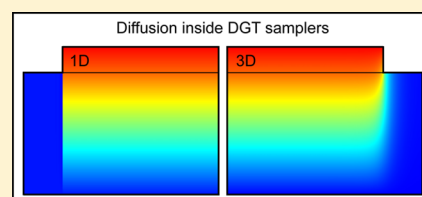
[†]University of Natural Resources and Life Sciences, Vienna, Department of Forest and Soil Sciences, Institute of Soil Research, Konrad-Lorenz-Strasse 24, 3430 Tulln an der Donau, Austria

[‡]Land Salzburg, Abteilung 5-Natur-und Umweltschutz, Gewerbe, Michael-Pacher-Straße 36, 5020 Salzburg, Austria

[§]Forschungszentrum Jülich IBG-3, Wilhelm-Johnen-Straße, 52425 Jülich, Germany

Supporting Information

ABSTRACT: Using numerical simulation of diffusion inside diffusive gradients in thin films (DGT) samplers, we show that the effect of lateral diffusion inside the sampler on the solute flux into the sampler is a nonlinear function of the diffusion layer thickness and the physical sampling window size. In contrast, earlier work concluded that this effect was constant irrespective of parameters of the sampler geometry. The flux increase caused by lateral diffusion inside the sampler was determined to be ~8.8% for standard samplers, which is considerably lower than the previous estimate of ~20%. Lateral diffusion is also propagated to the diffusive boundary layer (DBL), where it leads to a slightly stronger decrease in the mass uptake than suggested by the common 1D diffusion model that is applied for evaluating DGT results. We introduce a simple correction procedure for lateral diffusion and demonstrate how the effect of lateral diffusion on diffusion in the DBL can be accounted for. These corrections often result in better estimates of the DBL thickness (δ) and the DGT-measured concentration than earlier approaches and will contribute to more accurate concentration measurements in solute monitoring in waters.



INTRODUCTION

A DGT sampling unit consists of a resin gel, covered by a diffusive gel with a defined thickness and a protective membrane, all of which are enclosed in a sampler housing.^{1,2} The sampling process is simple: once the DGT device gets in contact with the sampled medium, the target solutes diffuse into the sampler where they get bound by the resin gel. On the basis of the 1D steady-state solution of Fick's first law of diffusion

$$J = \frac{D_{\text{gel}}(c_b - c_r)}{\Delta g} \quad (1)$$

the solute concentration at the sampler–medium interface can be calculated by eq 2¹

$$c_{\text{DGT}} = \frac{M \Delta g}{D_{\text{gel}} A_{\text{phys}} t} \quad (2)$$

Here, J is the diffusive flux, D_{gel} is the solute diffusion coefficient in the diffusion layer, c_b is the concentration in the exterior solution, c_r is the concentration in the resin gel (which is effectively zero as the resin is a strong solute sink), Δg is the diffusion layer thickness, c_{DGT} is the concentration at the sampler–medium interface, M is the mass of solute bound by the resin layer, A_{phys} is the physical sampling window surface area and t is the sampling time. When DGT was developed, c_{DGT} was considered a measure of c_b , based on the assumptions that either only one diffusing solute species exists or that all species have the same diffusion coefficient and are equally

strongly bound by the binding material (e.g., differently protonated species), that the diffusive boundary layer (DBL) forming outside the protective membrane has negligible effect on the sampler's mass uptake in well-stirred laboratory solutions and agitated natural waters,¹ and, implicitly, that diffusion inside the sampler is one-dimensional and has no lateral components.

In an investigation of phosphate fluxes in an eutrophic pond the DBL was, however, found to significantly decrease the solute uptake.³ In this study the DBL thickness, δ , was estimated by deploying DGT samplers with varying diffusive layer thicknesses and evaluating a plot of the reciprocal mass ($1/M$) versus Δg . Therefore, separate terms for solute diffusion in the DBL and the filter membrane layer were integrated into the DGT equation^{3,4}

$$c_b^{\text{DGT}} = \frac{M}{A_{\text{phys}} t} \left(\frac{\Delta g}{D_{\text{gel}}} + \frac{\Delta f}{D_f} + \frac{\delta}{D_{\text{water}}} \right) \quad (3)$$

The superscript DGT indicates a c_b estimate obtained using DGT. In eq 3, Δf represents the thickness of the membrane and D_f and D_{water} are the diffusion coefficients in the membrane layer and in water. For standard, APA2-type diffusion gels⁵ and Supor membranes (Pall Corporation, Port Washington, NY,

Received: January 9, 2015

Revised: April 10, 2015

Accepted: April 15, 2015

Published: April 15, 2015

USA), for which diffusion coefficients were reported to be indistinguishable,⁶ the membrane thickness can be added to Δg and the term for the membrane can be omitted. Note that eq 3 provides a measure of c_b , as the effect of the DBL on solute mass uptake is corrected for.

Using A_{phys} for evaluating their experimental results, Warnken et al.⁷ observed systematically higher c_b^{DGT} values compared to c_b after correcting for the DBL-related mass uptake decrease. High-resolution analysis of dried resin gels using laser ablation inductively coupled plasma mass spectrometry (LA-ICPMS) showed that this unexpectedly high mass uptake was caused by lateral solute diffusion inside the DGT samplers. The authors concluded that the DBL-related decrease in mass uptake is balanced by the increase caused by lateral solute diffusion for standard DGT devices ($\Delta g = 0.94$ mm, $A_{\text{phys}} = 3.14$ cm²) deployed in well-stirred solutions. In this case, the simplification of using the physical sampling window area ($A_{\text{phys}} = 3.14$ cm²) and the simple DGT equation was found to be acceptable.⁷ For cases where no balancing of the two effects can be expected, Warnken et al.⁷ suggested to use the expanded DGT equation and an effective sampling area (A_{eff}) instead of the physical sampling window area to account for the lateral diffusion effect. A general flux increase of $\sim 20\%$ was adopted for DGT samplers, translating to $A_{\text{eff}} = 3.80$ cm² for standard DGT devices ($A_{\text{phys}} = 3.14$ cm²) and $A_{\text{eff}} = 3.08$ cm² for DGT devices with smaller physical window area ($A_{\text{phys}} = 2.54$ cm²).⁷

In this and in subsequent studies^{8–11} the relative flux increase due to lateral diffusion was assumed to be constant irrespective of the sampler geometry (e.g., Δg , A_{phys}). Only very recently, Garmo¹² presented modeling data indicating that the previous A_{eff} estimate for samplers with $r_{\text{phys}} = 0.9$ cm is too low, and that there might be an effect of A_{phys} on A_{eff} . A sketch of a DGT sampler shows that lateral diffusion inside the sampler takes place at the edge of the diffusion and resin gels, where the sampler housing extends over the diffusion layer (Figure 1). The solute binding by the underlying resin gel drives the

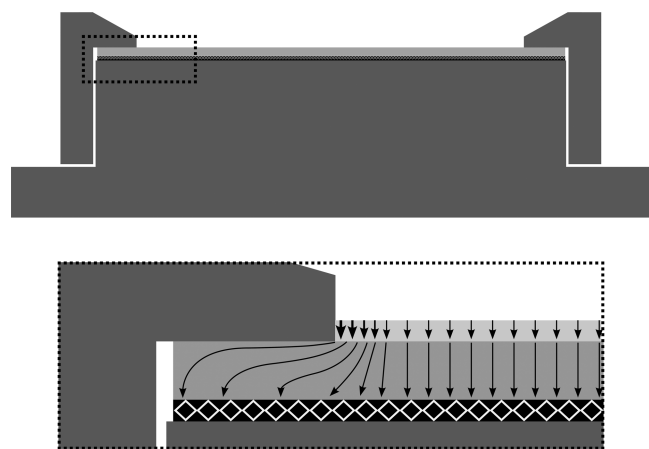


Figure 1. Illustration of solute diffusion inside a DGT sampler. The DGT sampler housing covers a ~ 2.5 mm wide area of the diffusion layer and the resin gel. The direction of the concentration gradient that establishes at the edge of the sampler is oriented toward the resin gel edge, as the solute concentration in this area is lower than in the diffusion layer zone that is in direct contact with the medium. As a consequence, the solute concentration at the diffusion layer–DBL interface is lower than in the center of the sampler, leading to a higher solute flux into the sampler at the sampler edge compared to the center.

outward, lateral flux of solute in this region. Figure 1 indicates that the diffusion layer thickness, but also the size of the covered gel region (i.e., the physical sampler window area) might affect the concentration gradient and thereby the magnitude of the flux increase because of lateral diffusion, hence A_{eff} should depend on the sampler geometry.

In this study, we apply numerical modeling for simulating 3D diffusion into and inside DGT samplers to investigate the dependence of the lateral diffusion-induced mass uptake increase on Δg and A_{phys} . Moreover, we strive for identifying additional parameters that might affect the solute flux into and inside DGT samplers.

MATERIALS AND METHODS

Model. DGT samplers are circular devices, therefore three-dimensional solute diffusion inside and into DGT devices can be reduced to a 2D-axisymmetric problem. We solved the diffusion equation (eqs S1, S6, and S7 in the Supporting Information) on two different, 2D-axisymmetric simulation geometries, one representing the diffusion layer without considering the DBL (Supporting Information Figure S1 top) and a second including the overlying DBL layer (Supporting Information Figure S1 bottom). In the first case, only the diffusion coefficient in the diffusion gel, D_{gel} , was considered, while in the second case D_{water} was additionally used as diffusion coefficient in the DBL. The complete description of the mathematical problem is given in the Supporting Information.

The flux profiles into the resin gel that were obtained from the 2D-axisymmetric model were used to create revolution surfaces, across which the flux into the resin gel was integrated to obtain the cumulated solute flux into the DGT sampler. Although, strictly, the results reported in this study are based on 2D-axisymmetric simulations, they are a valid representation of the 3D solute flux into the sampler. Therefore, our results are addressed as '3D' results in the following.

The sampling window had radii r_{phys} of 1.0 and 0.9 cm (standard DGT sampler sizes for solution and soil sampling), the resin gel disc radius (r_{gel}) was 1.25 cm. The diffusion layer thickness Δg was varied between 0.001 cm, as used in chemical imaging studies,^{13,14} and 0.5 cm as upper extreme value. The diffusion boundary layer thickness (δ) was varied between 0.0025 and 0.1 cm. Phosphate (H_2PO_4^-) was used as model solute unless stated otherwise. A value of $D_{\text{water}} = 8.47 \times 10^{-6}$ cm² s⁻¹ (25 °C) was adopted as diffusion coefficient in water¹⁵ and $D_{\text{gel}} = 6.05 \times 10^{-6}$ cm² s⁻¹ (25 °C) was adopted as diffusion coefficient in the diffusion layer.³ The exterior solution concentration of phosphate (c_b) was set to 100 nmol L⁻¹. An overview on model parameters and parameter values is given in Supporting Information Table S1.

A steady solute flux into a DGT sampler is established a few minutes after exposure of the sampler to the sampled medium.¹ Throughout this study, stationary solutions of the model were used to evaluate the diffusional behavior after this initial phase of flux establishment. All simulations were done using the Earth Science Module of the Comsol 4.0a package (Comsol Multiphysics GmbH, Göttingen, Germany).

Lateral Diffusion Inside the Sampler. Lateral diffusion inside the sampler was evaluated by comparing simulated 3D fluxes into DGT samplers without DBL, which include the lateral diffusion effect, to fluxes calculated using the 1D solution for the DGT flux¹

Table 1. Simulated Phosphate Fluxes into DGT Samplers

Δg (cm)	1D flux $\delta = 0 \mu\text{m}$ (nmol s ⁻¹)	3D flux $\delta = 0 \mu\text{m}$ (nmol s ⁻¹)	flux in- crease ^a (%)	1D flux $\delta = 100 \mu\text{m}$ (nmol s ⁻¹)	1D flux $\delta = 200 \mu\text{m}$ (nmol s ⁻¹)	3D flux $\delta = 100 \mu\text{m}$ (nmol s ⁻¹)	3D flux $\delta = 200 \mu\text{m}$ (nmol s ⁻¹)
$r_{\text{phys}} = 1 \text{ cm}$							
0.001	1900.7	1902.5	0.10	233.4	124.3	233.4	124.3
0.005	380.1	382.1	0.51	156.5	98.6	156.8	98.6
0.020	95.0	97.0	2.06	70.0	55.4	70.8	55.9
0.054	35.2	37.0	5.10	31.1	27.8	32.3	28.7
0.094	20.2	22.0	8.75	18.8	17.6	20.1	18.7
0.200	9.5	11.2	18.14	9.2	8.9	10.7	10.2
0.500	3.8	5.1	34.77	3.7	3.7	5.0	4.9
$r_{\text{phys}} = 0.9 \text{ cm}$							
0.001	1539.5	1541.1	0.10	189.1	100.7	189.0	100.7
0.005	307.9	309.7	0.59	126.8	79.8	127.0	79.9
0.020	77.0	78.7	2.29	56.7	44.9	57.5	45.3
0.054	28.5	30.1	5.68	25.2	22.5	26.3	23.4
0.094	16.4	18.0	9.74	15.2	14.2	16.4	15.2
0.200	7.7	9.3	20.72	7.4	7.2	8.8	8.4
0.500	3.1	4.5	45.87	3.0	3.0	4.4	4.3

^aOnly accounting for lateral diffusion (columns 2 and 3), not for the DBL.

$$f_{\text{DGT}} = \frac{A_{\text{phys}} D_{\text{gel}} c_b}{\Delta g} \quad (4)$$

disregarding the effect of lateral diffusion at the sampler edges.

Effect of the DBL. For investigating the effect of the DBL on the sampler flux, simulation runs with varying diffusion layer and DBL thicknesses were conducted. These sampler fluxes were compared to 1D fluxes without DBL (eq 4) and to 1D fluxes including the DBL, which were simulated with a simple 1D representation of the DGT geometry. In addition, the effects of different sampling window surface areas and different diffusion coefficients, using literature values for H_2PO_4^- , H_2AsO_4^- , and Cd^{2+} ,^{1,3,15,16} (Supporting Information Table S1) were investigated.

Correction for Lateral Diffusion in Estimations of the DBL Thickness Using DGT. To date, the constant correction coefficient A_{eff} ⁷ is used to account for lateral diffusion in DGT measurements. Here we investigate the effect of applying the nonconstant correction coefficients determined in this study on the results of DBL thickness estimations using (1) a simulated data set and (2) literature data. The literature data was digitized from Figure 2a in Garmo et al.⁸ and Figure 2b in Warnken et al.⁷ using the free software “Plot Digitizer” (<http://sourceforge.net/projects/plotdigitizer>).

The DBL thickness (along with c_b) can be determined by fitting eq 5,

$$M = \frac{A_{\text{eff}} t c_b}{\frac{\Delta g}{D_{\text{gel}}} + \frac{\delta}{D_{\text{water}}}} \quad (5)$$

representing the expanded DGT equation (eq 3) solved for M , to DGT-determined solute masses M . For simplifying the fitting procedure a linearized version of eq 5, Supporting Information eq S14, has been used.^{3,7} Parameter estimation using linearized data that might be affected with random measurement errors of constant magnitude may however be biased, as the contribution of the error increases as the data value decreases.¹⁷ To avoid such bias, Garmo et al.⁸ proposed

to fit M directly to the nonlinearized DGT equation, which is convenient with modern office software packages. Furthermore, Garmo et al.⁸ modified the expanded DGT model (eqs 3, 5) to include both, the physical sampler window surface area A_{phys} and the effective area A_{eff}

$$M = \frac{A_{\text{eff}} A_{\text{phys}} D_{\text{water}} D_{\text{gel}} t c_b}{A_{\text{eff}} D_{\text{gel}} \delta + A_{\text{phys}} D_{\text{water}} \Delta g} \quad (6)$$

to better account for lateral diffusion. In this study we estimated δ and c_b using both, eqs 5 and 6. Fits of these equations to the simulated and literature data sets were computed using (1) $A_{\text{eff}} = 3.8 \text{ cm}^2$ or $A_{\text{eff}} = 3.08 \text{ cm}^2$, as appropriate,⁷ (2) correction for lateral diffusion inside the sampler only (k_{LD} , explanation in Results and Discussion), and (3) correction for lateral diffusion and non-1D diffusion through the DBL (k_{LD} and k_{DBL} , explanation in Results and Discussion).

RESULTS AND DISCUSSION

Lateral Diffusion Inside the Sampler. Table 1 shows 1D and 3D phosphate fluxes into DGT samplers with different diffusion layer thicknesses. Considering only the fluxes computed without DBL it is evident that the 3D fluxes are always higher than the 1D fluxes, with the flux difference increasing with increasing Δg . The reason for this flux increase, as already outlined in the introduction and visualized in Figure 1, is the lateral diffusion at the sampler edges, which has already been shown experimentally by Warnken et al.⁷ Simulated profiles of the solute flux into the resin gel show that an increasing solute mass fraction is transported toward the edge of the resin gel upon increasing the diffusion layer thickness (Supporting Information Figure S2). For very small Δg values (0.001 cm, 0.005 cm), the outward solute flux is negligible, and the area of resin gel that receives solute corresponds largely to the physical sampler window surface area. When using thicker diffusion layers more solute diffuses outward, increasing the resin gel area that receives solute. It can be seen that the central area of the resin gel receives solute corresponding to the 1D

flux for most diffusion layer thicknesses used here, with this central resin gel area becoming smaller with increasing diffusion layer thickness. Only for extremely thick diffusion layers ($\Delta g = 0.5$ cm) the solute flux to the resin gel decreases to below the 1D situation even in the very center of the sampler. The flux increases predicted by the model range from 0.1% to 34.5% for samplers with $r_{\text{phys}} = 1.0$ cm and from 0.1% to 45.9% for $r_{\text{phys}} = 0.9$ cm (Table 1), showing that not only the diffusion layer thickness, but also the size of the sampler window affects lateral diffusion.

Correction for Lateral Diffusion Inside the Sampler. It has been suggested to use the effective sampling area (A_{eff}) instead of the physical sampling surface area (A_{phys}) to correct for lateral diffusion when applying eq 3, that is, in situations where the flux increase that is brought about by lateral diffusion is not balanced by the flux decrease because of the formation of the DBL.⁷ In the special case that both effects balance each other, eq 2 can be used. The result for both situations is that $c_b^{\text{DGT}}/c_b \approx 1$, so DGT provides a measurement of the solute concentration in the exterior solution. This mathematical correction of lateral diffusion is necessary because DGT results are evaluated using a 1D solution of Fick's law of diffusion, while the sampling process is based on omnidirectional (3D) diffusion. As the standard 1D equation (eq 2) works well unless the DBL and lateral diffusion effects do not balance each other, the need for correcting for lateral diffusion has been recognized relatively late.

As lateral diffusion depends on the sampler geometry, the sampler geometry has to be accounted for when correcting for lateral diffusion. The lateral diffusion flux increase coefficient, k_{LD} , can be defined as the ratio of the solute flux into the sampler in the 3D situation, $f_{0,3\text{D}}$, and the 1D flux, $f_{0,1\text{D}}$

$$k_{\text{LD}} = \frac{f_{0,3\text{D}}}{f_{0,1\text{D}}} \quad (7)$$

Here, the index "0" indicates a DBL layer thickness of $\delta = 0$ (cf., definition of k_{DBL} , eq 11). A plot of k_{LD} versus Δg for samplers with r_{phys} values of 0.9 and 1.0 cm shows a nonlinear relation of the two parameters (Figure 2). Second-order polynomial functions result in excellent fits ($r^2 = 0.9998$ and 0.9999, respectively) to these data.

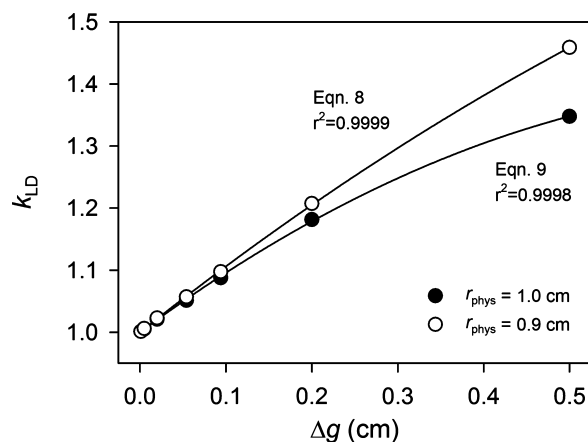


Figure 2. Lateral diffusion correction factor k_{LD} versus Δg . The data points are results of simulation runs, the lines are fits of second-order polynomial functions to the simulated data.

$$k_{\text{LD}} = -0.360\Delta g^2 + 1.098\Delta g + 1 \text{ for } r_{\text{phys}} = 0.9 \text{ cm} \quad (8)$$

$$k_{\text{LD}} = -0.658\Delta g^2 + 1.025\Delta g + 1 \text{ for } r_{\text{phys}} = 1.0 \text{ cm} \quad (9)$$

Therefore, eqs 8 and 9 can be used to determine the flux increase coefficient for a given diffusion layer thickness and correcting c_b^{DGT} for lateral diffusion through dividing by the flux increase factor

$$c_b^{\text{DGT}} = \frac{M}{k_{\text{LD}}A_{\text{phys}}t} \left(\frac{\Delta g}{D_{\text{gel}}} + \frac{\Delta f}{D_f} + \frac{\delta}{D_{\text{water}}} \right) \quad (10)$$

Solute Diffusion in the DBL. The geometry of the model DBL used in this study is idealized with respect to the DBL being equally thick throughout the whole solution-sampler interface (Figure 1 and Supporting Information Figure S1), however, this simplification is consistent with DGT theory.^{1,3,7,8} The physical DBL that forms around a DGT sampler in a solution will have a different shape, i.e. a thicker DBL layer toward the edges of the sampling window and a thinner one toward the center can be expected, therefore the DBL thickness estimated using DGT samplers is an average value across the sampler surface.¹⁸

Table 1 shows simulated DGT fluxes with and without DBL layers ($\delta = 100$ and $200 \mu\text{m}$), which indicate that the increased flux because of lateral diffusion into DGT samplers with a common diffusion layer thickness of 0.094 cm (i.e., a flux increase of 8.7–9.7%) is balanced by DBL layers of $\sim 100 \mu\text{m}$ thickness for r_{phys} values of 1 and 0.9 cm. This observation is in line with the general finding that $c_b^{\text{DGT}}/c_{\text{soln}} \approx 1$ for $\Delta g = 0.094$ cm in well-stirred solutions, as reported in earlier studies.^{1–3,13,19} In contrast, Warnken et al.⁷ reported DBL layer thicknesses of $230 \pm 32 \mu\text{m}$ in moderate to well stirred solutions, which did not change upon varying the solution flow velocity (i.e., stir rate), and matched well with their estimation of the lateral diffusion flux increase of $\sim 20\%$.

Simulation runs with and without DBL were performed for investigating the effect of solute species (D_{water} , D_{gel}), r_{phys} , Δg , and δ on solute diffusion through the DBL. As we expected the ratio of the diffusion coefficients, $D_{\text{gel}}/D_{\text{water}}$, to determine the effect of the diffusion coefficient, arsenate ($D_{\text{water}} = 9.05 \times 10^{-6} \text{ cm}^2 \text{ s}^{-1}$, $D_{\text{gel}} = 5.93 \times 10^{-6} \text{ cm}^2 \text{ s}^{-1}$)^{15,16} and Cd ($D_{\text{water}} = 7.17 \times 10^{-6} \text{ cm}^2 \text{ s}^{-1}$, $D_{\text{gel}} = 6.09 \times 10^{-6} \text{ cm}^2 \text{ s}^{-1}$)^{6,15,20} were chosen as additional solutes to cover a wide range of $D_{\text{gel}}/D_{\text{water}}$ ratios. Potential differences in the flux decrease due to the DBL in the 1D and 3D situation were evaluated using

$$k_{\text{DBL}} = \frac{\frac{f_{\text{DBL},3\text{D}}}{f_{0,3\text{D}}}}{\frac{f_{\text{DBL},1\text{D}}}{f_{0,1\text{D}}}} \quad (11)$$

where the index DBL denotes a specific DBL thickness, while the index "0" denotes $\delta = 0$. f_{DBL}/f_0 is the sampler flux decrease caused by the presence of the DBL. By normalizing the sampler flux decrease in the 3D situation for that in 1D, k_{DBL} provides a measure of how much the sampler flux is changed in the 3D geometry compared to the common 1D solutions of the DGT equation.

A plot of k_{DBL} vs. $D_{\text{gel}}/D_{\text{water}}$ shows that the DBL flux decrease in 3D is ~ 0.95 – 0.99 times the flux decrease of the 1D situation ($r_{\text{phys}} = 1$ cm, $\Delta g = 0.094$ cm; Figure 3) and that there is a slight dependence of the magnitude of the flux decrease on the solute species (i.e., $D_{\text{gel}}/D_{\text{water}}$). k_{DBL} also depends on Δg

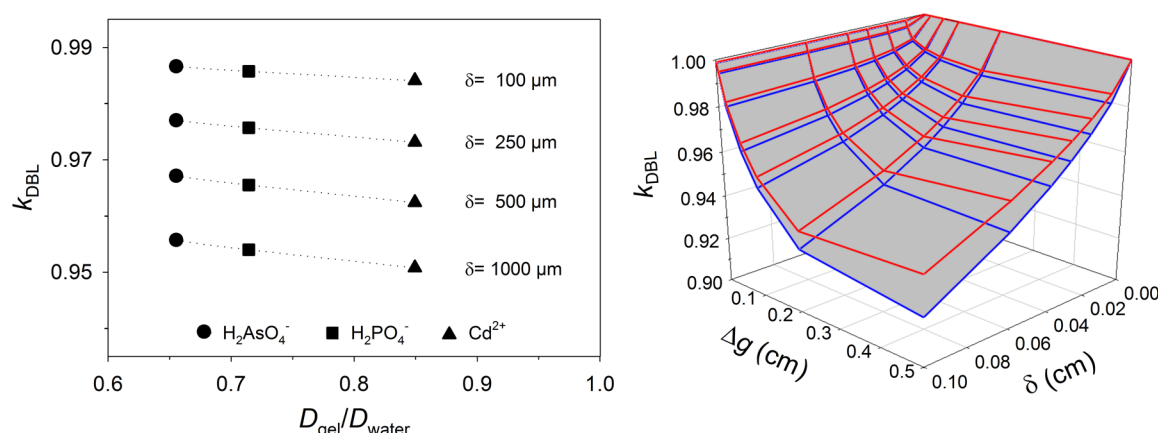


Figure 3. Parameters affecting the DBL related flux decrease (k_{DBL}). Left: Dependence of k_{DBL} on $D_{\text{gel}}/D_{\text{water}}$, which is a solute species-specific ratio. Right: Effect of Δg , δ , and r_{phys} on k_{DBL} . Red lines: $r_{\text{phys}} = 1.0$ cm. Blue lines: $r_{\text{phys}} = 0.9$ cm.

and δ , with extreme values of $k_{\text{DBL}} = 0.93$ ($r_{\text{phys}} = 1.0$ cm) and $k_{\text{DBL}} = 0.92$ ($r_{\text{phys}} = 0.9$ cm) for $\Delta g = 0.5$ cm and $\delta = 0.1$ cm. This shows that the flux decrease associated with the formation of the DBL is larger when 3D diffusion is considered, as compared to the 1D situation, and that k_{DBL} is dependent on numerous parameters ($D_{\text{water}}/D_{\text{gel}}$, r_{phys} , Δg , δ).

Correction for Non-1D Diffusion in the DBL. The slight difference in the DBL-related flux decrease between 1D and 3D diffusion in the order of a few percent effectively is a propagation of the effect of lateral diffusion inside the sampler to the diffusive regime outside. The concentration gradient that causes the outward diffusion of solutes inside the sampler affects diffusion in the DBL as the solute concentration at the sampler-solution interface at the edge of the sampling window will be smaller than the concentration at the center of the interface. This or similar effects have recently been hypothesized by Davison and Zhang.¹⁸

In principle, the difference in solute diffusion through the DBL in 1D and 3D can be corrected for in the full DGT equation by introducing k_{DBL} as a further correction factor

$$c_{\text{b}}^{\text{DGT}} = \frac{M}{k_{\text{LD}} k_{\text{DBL}} A_{\text{phys}} t} \left(\frac{\Delta g}{D_{\text{gel}}} + \frac{\Delta f}{D_{\text{f}}} + \frac{\delta}{D_{\text{water}}} \right) \quad (12)$$

however, this would require knowledge, or at least a good estimate, of the DBL thickness before k_{DBL} can be determined. Moreover, given the number of controlling parameters, it would be necessary to determine k_{DBL} for each individual DGT deployment by numerical simulation similar to this study. As doing so is rather impractical and as the error by neglecting this correction step is small (see DBL Thickness Estimation section) k_{DBL} could be omitted in most studies. Therefore, eq 10 might serve as standard equation to account for lateral diffusion only inside the sampler.

Differential Appreciation of Lateral Diffusion by This and Earlier Work. The conclusions of the present study and those of Warnken et al.⁷ on the effect of lateral diffusion and the DBL on DGT measurements differ considerably. In the earlier work a lateral diffusion-related relative flux increase of ~20% was estimated, which was considered to be independent of the diffusion layer thickness as well as of the sampling window surface area. This earlier study is an elaborate, extensive treatment of lateral diffusion inside DGT samplers, therefore it is interesting to analyze why its results and conclusions differ from those presented here.

Direct evidence for lateral diffusion inside DGT samplers was obtained in Warnken et al.⁷ by measuring the Cd distribution across a DGT resin gel disk that was immersed in a Cd-containing solution with a diffusion layer thickness of 0.134 cm using LA-ICPMS. The obtained Cd profile showed shoulders at the edges of the gel disk, consistent with outward diffusion of Cd. From this profile, the authors calculated the effective gel radius, that is, the profile length necessary to explain the additional Cd uptake on the basis of 1D diffusion. This resulted in an effective gel radius of 1.08 cm, which corresponds to an effective area of 3.66 cm² or a relative flux increase of ~17%.

The quantification of the lateral diffusion-based flux increase was based on a different approach. Therefore, Warnken et al.⁷ corrected $c_{\text{b}}^{\text{DGT}}$ values for the DBL effect, which should result in $c_{\text{b}}^{\text{DGT}}/c_{\text{b}} > 1$ if lateral diffusion increases solute uptake. This was achieved by immersing DGT samplers with different diffusion layer thicknesses in stirred laboratory solutions, plotting $1/M$ versus Δg , determining the slope and intercept of the resulting regression line, and calculating $c_{\text{b}}^{\text{DGT}}$ and δ using an earlier developed procedure.^{1,3,4} In one of those experiments, deploying four DGT samplers for 50 h in a Cd containing solution, Warnken et al.⁷ found a DBL thickness of 170 μm . The associated $c_{\text{b}}^{\text{DGT}}$ value, which should correspond to c_{b} , given that the DBL related flux decrease should be accounted for by the estimation procedure, was ~20% larger than the solution concentration. The increased mass uptake was considered an effect of lateral diffusion, as this effect is not covered by the applied fitting procedure. This reasoning is sound, provided that the procedure for estimating c_{b} and δ is correct and accurate.

Repeating this calculation using data digitized from the corresponding Figure 2b in Warnken et al.⁷ gives $c_{\text{b}}^{\text{DGT}} = 10.9 \mu\text{g L}^{-1}$, $\delta = 180 \mu\text{m}$, and $c_{\text{b}}^{\text{DGT}}/c_{\text{b}} = 1.16$, that is a lateral diffusion flux increase of ~16%. Considering the uncertainty associated with data digitalization and that the average c_{b} during the 50 h DGT deployment was not given in the paper (we estimated a value of $9.4 \mu\text{g L}^{-1}$ based on the available data), the agreement to the published values is very good. The individual $c_{\text{b}}^{\text{DGT}}$ values for all four samplers have a relative standard deviation (RSD) of 1.6% based on $\delta = 180 \mu\text{m}$, which is a minimum compared to lower or higher DBL values. Correction for the nonconstant, diffusion layer thickness-dependent flux increase (k_{LD}) gives an average $c_{\text{b}}^{\text{DGT}}$ of $9.7 \mu\text{g L}^{-1}$ and hence $c_{\text{b}}^{\text{DGT}}/c_{\text{b}} = 1.03$, consistent with a theoretical $c_{\text{b}}^{\text{DGT}}/c_{\text{b}} = 1$ after accounting for lateral diffusion. For this case the RSD of the

Table 2. Estimation of δ and c_b for DGT Measurements with Samplers of Different Diffusion Layer Thickness^a

initial parameters; correction method	full DGT model			modified DGT model ⁸		
	δ (μm)	c_b^{DGT} ($\mu\text{g L}^{-1}$)	r^2	δ (μm)	c_b^{DGT} ($\mu\text{g L}^{-1}$)	r^2
simulated data (this study)						
input parameters ^b	200	100				
A_{eff} (eqs 5, 6)	208	85.7	0.9999	172	85.7	0.9999
k_{LD} (Supporting Information eqs S15, S17)	196	97.9	1.0000	198	99.3	1.0000
k_{LD} and k_{DBL} (Supporting Information eqs S16, S18)	200	100.0	1.0000	202	100.8	1.0000
data set of Garmo et al.,⁸ Figure 2a						
c_b measured by authors					10.0	
estimated by authors				208	9.3	
A_{eff} (eqs 5, 6)	254	9.5	0.9950	210	9.5	0.9950
k_{LD} (Supporting Information eqs S15, S17)	207	10.1	0.9961	211	10.3	0.9961
k_{LD} and k_{DBL} (Supporting Information eqs S16, S18)	211	10.3	0.9961	216	10.5	0.9961
data set of Warnken et al.,⁷ Figure 2b						
c_b nominal by authors ^c		~ 10				
c_b estimated (this study) ^c		9.4				
estimated by authors ^c	170					
A_{eff} (eqs 5, 6)	188	9.2	0.9998	156	9.2	0.9998
k_{LD} (Supporting Information eqs S15, S17)	158	10.0	0.9993	160	10.2	0.9993
k_{LD} and k_{DBL} (Supporting Information eqs S16, S18)	161	10.2	0.9994	163	10.3	0.9994

^aThe DBL thickness and c_b were estimated by fitting eqs 5 and 6 to a simulated and two literature data sets. The effects of lateral diffusion and the DBL were corrected for by using A_{eff} , k_{LD} or k_{LD} and k_{DBL} . ^bInput parameters for creating the set of simulated data points. ^c" c_b nominal" is the approximate solute (Cd) concentration given in the paper; " c_b estimated" is the estimated, time-averaged Cd concentration during this 50 h experiment, based on the data given in the paper, see Materials and Methods section for details. ^dEstimated using the linearized version of the expanded DGT equation (Supporting Information eq S14).⁷

c_b^{DGT} values is lowest with 3.0% at $\delta = 140 \mu\text{m}$. The k_{LD} s used here ranged from 1.014 ($\Delta g = 0.014 \text{ cm}$) to 1.126 ($\Delta g = 0.134 \text{ cm}$), which is considerably less than the flux increase factor determined by Warnken et al.⁷ Following Zhang and Davison,¹ Warnken et al.⁷ assumed a linear relationship of $1/M$ vs. Δg , however the assumption of linearity does not hold if the lateral diffusion flux increase is a nonlinear function of Δg . Their procedure for estimating c_b and δ , based on evaluating the slope and intercept of a linear regression line, is therefore not rigorous and leads to different results for the DBL, and, based thereon, A_{eff} , compared to using nonconstant, nonlinear k_{LD} values.

In conclusion, using a constant flux increase factor (independent of the sampler geometry, i.e. of Δg , A_{phys}) resulted in the adoption of a relative flux increase of $\sim 20\%$. However, even if A_{eff} had been more accurately determined for an individual diffusion layer thickness it would have been very hard to establish nonconstant lateral diffusion induced flux increases based on experimental data, as the flux increases in the commonly used Δg range (0.02–0.2 cm) can easily be masked by the measurement uncertainty, which is often in the range of 5–10%.¹⁶

DBL Thickness Estimation. Table 2 shows the results of estimating δ and c_b using simulated and literature DGT measurements with varying Δg . The fits of the full DGT model to the simulated data resulted in deviations from the initial δ of up to only $\sim 4\%$ for all lateral diffusion correction methods (A_{eff} , k_{LD} or k_{LD} and k_{DBL}). However, c_b^{DGT} converged to the initial value only when k_{LD} and k_{LD} and k_{DBL} were employed, whereas using A_{eff} resulted in a deviation of $\sim -14\%$. The modified model of Garmo et al.⁸ resulted in decreased δ and c_b^{DGT} values

when using A_{eff} , both in the range of $\sim -14\%$, but performed equally well as the full model when applying k_{LD} and k_{LD} and k_{DBL} . The full model lead to perfect estimates for both, δ and c_b , when applying k_{LD} and k_{DBL} , which is of course expected for a simulated, measurement error-free data set. However, the model of Garmo et al.⁸ deviated by about 1% from to initial values, showing that their modification is no full representation of the DGT sampling process. Moreover, it does not lead to improved parameter estimates when applying A_{eff} which was the actual aim of introducing their modified model.

The δ estimates obtained by fits of the literature data to the full DGT model with A_{eff} correction are $\sim 20\%$ higher than the estimates obtained with k_{LD} and k_{LD} and k_{DBL} correction. The δ values obtained from the modified DGT model, irrespective of the correction method, are in the same range as the values obtained with the full DGT model and k_{LD} and k_{LD} and k_{DBL} correction. The fitted c_b^{DGT} values deviate from the measured⁸ and estimated⁷ solution concentrations by -5% to $+9.6\%$.

These example estimations of δ and c_b show that the lateral diffusion correction methods proposed here, based on the use of k_{LD} or, if available, k_{LD} and k_{DBL} , result in better estimates than directly fitting the full DGT equation using A_{eff} correction. The modified DGT model proposed by Garmo et al.⁸ resulted in similar parameter estimates compared to the DGT equation with k_{LD} and k_{LD} and k_{DBL} correction for the experimental data sets, but not for the simulated data set, indicating that the full DGT equation with k_{LD} and k_{LD} and k_{DBL} correction provides more reliable parameter estimates. The difference between δ and c_b estimates based on the expanded DGT equation and k_{LD} versus k_{LD} and k_{DBL} correction was small with 1.0% to 2.4%, therefore the use of k_{LD} without k_{DBL} seems acceptable given

the effort needed to determine k_{DBL} by numerical simulation for individual DGT applications.

General Appraisal. We show that δ and c_b estimates in DGT applications with samplers of varying diffusion layer thickness vary considerably for different estimation strategies. The expanded DGT equation (eq 5) in combination with the lateral diffusion correction factor k_{LD} with or without k_{DBL} resulted in the best c_b estimates for simulated and experimental data. Moreover, this procedure precisely estimated δ in a simulated data set where the initial DBL thickness is known. Estimates based on A_{eff} were considerably different to initial and measured values in several of the investigated cases. The results obtained using the modified equation (eq 6) were typically within $\sim 10\%$ of the best estimates. In the study of Garino et al.,⁸ estimates using the linearized version of the full DGT equation were up to 25% (c_b) and 83% (δ) larger than those based on direct, nonlinearized fits to their modified model, indicating that the use of the linearized estimation procedure may introduce large errors in c_b and δ estimates. Therefore, we propose to use direct fits of the nonlinearized form of eq 5, with k_{LD} as the lateral diffusion correction factor. The procedure presented here is expected to increase the accuracy of c_b measurements in environmental monitoring applications of labile solute in waterbodies and might furthermore be relevant for obtaining more accurate determinations of complex dissociation kinetics by DGT, where lateral diffusion correction and parameter estimation through data fitting is also applied.^{18,21,22}

So far, the effect of lateral diffusion was only considered for DGT measurements in solutions, but not for measurements of labile solutes in sediments and soils. In solutions diffusion and, if labile complexed species are present, complex dissociation are controlling the mass uptake of DGT samplers. In soils and sediments the porewater concentration of the dissolved species are usually controlled by sorption and dissolution-precipitation equilibria, with potential contributions from the dissociation of complexes, but not by diffusion into the sampler. For these reasons, only up to ~ 3.4 -fold increases in the mass uptake of Cu, Cd,²³ and P²⁴ by DGT from soil were measured when the concentration gradient into the sampler was ~ 95 -fold increased by decreasing the diffusion layer thicknesses from 0.094 to 0.001 cm. Given these relatively small mass uptake increases for large increases in solute demand, changes of DGT mass uptake from soil and sediments in response to a potential lateral diffusion flux increase by a factor of up to 1.45 will be hardly measurable as compared to the 1D diffusion situation. Mathematical correction of the lateral diffusion flux increases in soil and sediment DGT measurements should therefore not be necessary.

■ ASSOCIATED CONTENT

■ Supporting Information

Simulation geometry (2D-axisymmetric), model definition, overview on parameter values used in this study, supplementary equations, and dependence of solute flux profiles into the resin layer on the diffusion layer thickness Δg . This material is available free of charge via the Internet at <http://pubs.acs.org>.

■ AUTHOR INFORMATION

Corresponding Author

*E-mail: jakob.santner@boku.ac.at.

Author Contributions

J.S. and A.K. contributed equally.

Notes

The authors declare no competing financial interest.

■ ACKNOWLEDGMENTS

We acknowledge the funding by the Austrian Science Fund (FWF): P23798-B16.

■ REFERENCES

- (1) Zhang, H.; Davison, W. Performance characteristics of diffusion gradients in thin films for the in situ measurement of trace metals in aqueous solution. *Anal. Chem.* **1995**, *67* (19), 3391–3400.
- (2) Davison, W.; Zhang, H. In situ speciation measurements of trace components in natural waters using thin-film gels. *Nature* **1994**, *367* (6463), 546–548.
- (3) Zhang, H.; Davison, W.; Gadi, R.; Kobayashi, T. In situ measurement of dissolved phosphorus in natural waters using DGT. *Anal. Chim. Acta* **1998**, *370* (1), 29–38.
- (4) Davison, W.; Fones, G. R.; Harper, M. P.; Teasdale, P. R.; Zhang, H. Dialysis, DET and DGT: In Situ Diffusional Techniques for Studying Water, Sediments and Soils. In *In Situ Monitoring of Aquatic Systems: Chemical Analysis and Speciation*; Buffle, J., Horvai, G., Eds.; Wiley: Chichester, U.K., 2000; pp 495–570.
- (5) Zhang, H.; Davison, W. Diffusional characteristics of hydrogels used in DGT and DET techniques. *Anal. Chim. Acta* **1999**, *398* (2–3), 329–340.
- (6) Scally, S.; Davison, W.; Zhang, H. Diffusion coefficients of metals and metal complexes in hydrogels used in diffusive gradients in thin films. *Anal. Chim. Acta* **2006**, *558* (1–2), 222–229.
- (7) Warnken, K. W.; Zhang, H.; Davison, W. Accuracy of the diffusive gradients in thin-films technique: Diffusive boundary layer and effective sampling area considerations. *Anal. Chem.* **2006**, *78* (11), 3780–3787.
- (8) Garino, Ø. A.; Naqvi, K. R.; Royset, O.; Steinnes, E. Estimation of diffusive boundary layer thickness in studies involving diffusive gradients in thin films (DGT). *Anal. Bioanal. Chem.* **2006**, *386* (7–8), 2233–2237.
- (9) Buzier, R.; Charriau, A.; Corona, D.; Lenain, J. F.; Fondanèche, P.; Joussein, E.; Poulier, G.; Lissalde, S.; Mazzella, N.; Guibaud, G. DGT-labile As, Cd, Cu and Ni monitoring in freshwater: Toward a framework for interpretation of in situ deployment. *Environ. Pollut.* **2014**, *192*, 52–58.
- (10) Turner, G. S. C.; Mills, G. A.; Bowes, M. J.; Burnett, J. L.; Amos, S.; Fones, G. R. Evaluation of DGT as a long-term water quality monitoring tool in natural waters: Uranium as a case study. *Environ. Sci.: Processes Impacts* **2014**, *16* (3), 393–403.
- (11) Uher, E.; Tusseau-Vuillemin, M. H.; Gourlay-France, C. DGT measurement in low flow conditions: Diffusive boundary layer and lability considerations. *Env. Sci. Process. Impact* **2013**, *15* (7), 1351–1358.
- (12) Garino, Ø. A. Simulating the effects of lateral diffusion and diffusive boundary layer on uptake in solution and soil type DGTs. Presented at the Conference on DGT and the Environment, 8–11 July 2013.
- (13) Kreuzeder, A.; Santner, J.; Prohaska, T.; Wenzel, W. W. Gel for Simultaneous Chemical Imaging of Anionic and Cationic Solutes Using Diffusive Gradients in Thin Films. *Anal. Chem.* **2013**, *85* (24), 12028–12036.
- (14) Williams, P. N.; Santner, J.; Larsen, M.; Lehto, N. J.; Oburger, E.; Wenzel, W.; Glud, R. N.; Davison, W.; Zhang, H. Localized flux maxima of arsenic, lead, and iron around root apices in flooded lowland rice. *Environ. Sci. Technol.* **2014**, *48* (15), 8498–8506.
- (15) Li, Y.-H.; Gregory, S. Diffusion of ions in sea water and in deep sea-sediments. *Geochim. Cosmochim. Acta* **1974**, *38*, 703–714.
- (16) Kreuzeder, A.; Santner, J.; Zhang, H.; Prohaska, T.; Wenzel, W. W. Uncertainty Evaluation of the Diffusive Gradients in Thin Films Technique. *Environ. Sci. Technol.* **2015**, *49* (3), 1594–1602.

- (17) Dowd, J. E.; Riggs, D. S. A Comparison of Estimates of Michaelis–Menten Kinetic Constants from Various Linear Transformations. *J. Biol. Chem.* **1965**, *240*, 863–869.
- (18) Davison, W.; Zhang, H. Progress in understanding the use of diffusive gradients in thin films (DGT) back to basics. *Environ. Chem.* **2012**, *9* (1), 1–13.
- (19) Santner, J.; Prohaska, T.; Luo, J.; Zhang, H. Ferrihydrite Containing Gel for Chemical Imaging of Labile Phosphate Species in Sediments and Soils Using Diffusive Gradients in Thin Films. *Anal. Chem.* **2010**, *82* (18), 7668–7674.
- (20) Zhang, H. DGT Manual. <http://www.dgtresearch.com/dgtresearch/dgtresearch.pdf> (accessed 11.11.2014).
- (21) Warnken, K. W.; Davison, W.; Zhang, H.; Galceran, J.; Puy, J. In situ measurements of metal complex exchange kinetics in freshwater. *Environ. Sci. Technol.* **2007**, *41* (9), 3179–3185.
- (22) Warnken, K. W.; Davison, W.; Zhang, H. Interpretation of in situ speciation measurements of inorganic and organically complexed trace metals in freshwater by DGT. *Environ. Sci. Technol.* **2008**, *42* (18), 6903–6909.
- (23) Lehto, N. J.; Davison, W.; Zhang, H. The use of ultra-thin diffusive gradients in thin-films (DGT) devices for the analysis of trace metal dynamics in soils and sediments: A measurement and modelling approach. *Environ. Chem.* **2012**, *9* (4), 415–423.
- (24) Santner, J.; Larsen, M.; Kreuzeder, A.; Glud, R. N. Two decades of chemical imaging of solutes in sediments and soils—A review. *Anal. Chim. Acta* **2015**, DOI: 10.1016/j.aca.2015.02.006.